



## OPEN ACCESS

## EDITED BY

Eleonora Vannini,  
Institute of Neuroscience (CNR), Italy

## REVIEWED BY

Amandine Grimm,  
University of Basel, Switzerland  
Beatrice D'Orsi,  
Institute of Neuroscience (CNR), Italy

## \*CORRESPONDENCE

Seok-Kyu Kwon  
skkwon@kist.re.kr  
Tommy L. Lewis Jr.  
tommy-lewis@omrf.org

†These authors have contributed  
equally to this work

## SPECIALTY SECTION

This article was submitted to  
Methods and Model Organisms,  
a section of the journal  
Frontiers in Molecular Neuroscience

RECEIVED 12 September 2022

ACCEPTED 17 October 2022

PUBLISHED 02 November 2022



## CITATION

Kim SY, Strucinska K, Osei B, Han K,  
Kwon S-K and Lewis TL Jr (2022)  
Neuronal mitochondrial morphology  
is significantly affected by both  
fixative and oxygen level during  
perfusion.  
*Front. Mol. Neurosci.* 15:1042616.  
doi: 10.3389/fnmol.2022.1042616

## COPYRIGHT

© 2022 Kim, Strucinska, Osei, Han,  
Kwon and Lewis. This is an  
open-access article distributed under  
the terms of the [Creative Commons  
Attribution License \(CC BY\)](https://creativecommons.org/licenses/by/4.0/). The use,  
distribution or reproduction in other  
forums is permitted, provided the  
original author(s) and the copyright  
owner(s) are credited and that the  
original publication in this journal is  
cited, in accordance with accepted  
academic practice. No use, distribution  
or reproduction is permitted which  
does not comply with these terms.

# Neuronal mitochondrial morphology is significantly affected by both fixative and oxygen level during perfusion

Su Yeon Kim<sup>1,2†</sup>, Klaudia Strucinska<sup>3†</sup>, Bertha Osei<sup>3†</sup>,  
Kihoon Han<sup>2</sup>, Seok-Kyu Kwon <sup>1,4\*</sup> and  
Tommy L. Lewis Jr. <sup>3,5\*</sup>

<sup>1</sup>Brain Science Institute, Korea Institute of Science and Technology (KIST), Seoul, South Korea, <sup>2</sup>Department of Neuroscience, College of Medicine, Korea University, Seoul, South Korea, <sup>3</sup>Aging and Metabolism Research Program, Oklahoma Medical Research Foundation, Oklahoma City, OK, United States, <sup>4</sup>Division of Bio-Medical Science and Technology, KIST School, Korea University of Science and Technology (UST), Daejeon, South Korea, <sup>5</sup>Departments of Biochemistry & Molecular Biology, Neuroscience and Physiology, University of Oklahoma Health Sciences Center, Oklahoma City, OK, United States

Neurons in the brain have a uniquely polarized structure consisting of multiple dendrites and a single axon generated from a cell body. Interestingly, intracellular mitochondria also show strikingly polarized morphologies along the dendrites and axons: in cortical pyramidal neurons (PNs), dendritic mitochondria have a long and tubular shape, while axonal mitochondria are small and circular. Mitochondria play important roles in each compartment of the neuron by generating adenosine triphosphate (ATP) and buffering calcium, thereby affecting synaptic transmission and neuronal development. In addition, mitochondrial shape, and thereby function, is dynamically altered by environmental stressors such as oxidative stress or in various neurodegenerative diseases including Alzheimer's disease and Parkinson's disease. Although the importance of altered mitochondrial shape has been claimed by multiple studies, methods for studying this stress-sensitive organelle have not been standardized. Here we address pertinent steps that influence mitochondrial morphology during experimental processes. We demonstrate that fixative solutions containing only paraformaldehyde (PFA), or that introduce hypoxic conditions during the procedure, induce dramatic fragmentation of mitochondria both *in vitro* and *in vivo*. This disruption was not observed following the use of glutaraldehyde (GA) addition or oxygen supplementation, respectively. Finally, using pre-formed fibril  $\alpha$ -synuclein treated neurons, we show fixative choice can alter experimental outcomes. Specifically,  $\alpha$ -synuclein-induced mitochondrial remodeling could not be observed with PFA only fixation as fixation itself

caused mitochondrial fragmentation. Our study provides optimized methods for examining mitochondrial morphology in neurons and demonstrates that fixation conditions are critical when investigating the underlying cellular mechanisms involving mitochondria in physiological and neurodegenerative disease models.

#### KEYWORDS

mitochondria, neuron, fixation, perfusion, hypoxia

## Introduction

Neurons are unique cells with distinct sizes, highly complex morphologies, and the ability to transmit and receive electro-chemical messages. The process of neurotransmission requires vast amounts of energy in the form of adenosine triphosphate (ATP) (Rolfe and Brown, 1997). While the respective contributions of the various metabolic processes to supply this ATP are not fully understood in neurons, mitochondria play a vital role in the ability of neurons to properly regulate their energy needs, as well as other critical processes including  $\text{Ca}^{2+}$  handling, lipid biogenesis, and regulation of the apoptotic pathway (Fox et al., 1988; Belanger et al., 2011; Chandel, 2014; Diaz-Garcia and Yellen, 2019).

The recent explosion in techniques to label and visualize organelles with high spatial resolution has revealed that excitatory pyramidal neurons (PNs) appear to contain distinct mitochondrial subpopulations within their respective cellular compartments of the axon, soma, and dendrites. Axonal mitochondria are small, individual entities while dendrites contain mitochondria that are highly elongated and overlapping each other (Popov et al., 2005; Chang and Reynolds, 2006; Lewis et al., 2018; Rangaraju et al., 2019). Mitochondria within the soma display intermediate size and morphology between those found in the axons and dendrites (Faitg et al., 2021; Turner et al., 2022).

Although most previous data conform to this consensus, there are discrepancies in the range of sizes. We reported that in mouse layer 2/3 cortical PNs, dendritic mitochondrial length ranges from 1.31 to 13.28  $\mu\text{m}$  long, but only 0.45 to 1.13  $\mu\text{m}$  in axons (Lewis et al., 2018). However, other studies observed both shorter dendritic mitochondria in cortical neurons (Kimura and Murakami, 2014), or longer dendritic mitochondria in live imaged cultured hippocampal neurons (Rangaraju et al., 2019). In addition, a recent study presented the length of dendritic mitochondria as  $4.7 \pm 0.9 \mu\text{m}$  by 3D electron microscopy (EM) imaging, but  $\text{Ca}^{2+}$  transients in the mitochondrial matrix

extended to 15  $\mu\text{m}$  (Lin et al., 2019). The reason for these gaps in size has not yet been scrutinized.

Mitochondria are proposed to be critical sites of reduced efficiency and function during the processes of normal aging and pathogenic neurodegeneration (Swerdlow et al., 2014; Azzu and Valencak, 2017). A common observation across many different forms of neurodegenerative diseases (including Alzheimer's and Parkinson's diseases) suggests a significant reduction in mitochondria number and size as well as a loss of mitochondrial ultrastructure (Zhang et al., 2016; Gonzalez-Rodriguez et al., 2021). In addition, fragmented mitochondria are increased following cerebral ischemia (Owens et al., 2015; Zhou et al., 2021).

Based on our own observations, and the large variance in the reported sizes of dendritic mitochondria in PNs and fixation conditions in the literature, we hypothesized that standard fixation conditions may not faithfully capture the mitochondrial structure present in living neurons. Thus, we rigorously tested the effects of multiple fixation parameters on the morphology of mitochondria in both cultured primary PNs as well as PNs *in vivo*. We find that a combination of direct fixation with a mixture of paraformaldehyde (PFA) (2%) and glutaraldehyde (GA) (0.075%) with the presence of sufficient oxygen is critical for maintaining mitochondrial morphology during fixation *in vitro* and *in vivo*.

## Methods

### Animals

Animals were handled according to Institutional Animal Care and Use Committee (IACUC) approved protocols at the Oklahoma Medical Research Foundation (OMRF) and the Korea Institute of Science and Technology (KIST-2020-133). Time-pregnant females of the CD-1 IGS strain (Strain Code: 022) were purchased at Charles River Laboratories or Daehan Biolink (Eumseong, South Korea) and used for *in utero* electroporation (IUE) experiments and primary neuronal cultures.

Abbreviations: PN, pyramidal neuron; PFA, paraformaldehyde; GA, glutaraldehyde; ATP, adenosine triphosphate; EM, electron microscopy; EUE, *ex utero* electroporation; IUE, *in utero* electroporation.

## Plasmids

pCAG:mtYFP-P2A-tdTomato and pCAG:mt-YFP were previously published in Lewis et al. (2016). pCAG:Cre and pCAG:HA-mCherry were previously used in Kwon et al. (2016). pAAV EF1 $\alpha$ :Flex Venus-T2A-mito-mScarlet was created by replacing Synaptophysin-Venus to Venus-T2A-mito-mScarlet in pAAV EF1 $\alpha$ :Flex-Synaptophysin-Venus from Kwon et al. (2016).

## Cell lines

Mouse Embryonic Fibroblast (NIH/3T3) was purchased from ATCC (CRL-1658). A total of  $1 \times 10^5$  cells of NIH/3T3 cells suspended in media (DMEM, Gibco) with penicillin/streptomycin (0.5 $\times$ ; Gibco) and FBS (Sigma) were seeded on coverslips (Collagen Type I, Corning) in 6 well dishes. Transfection with plasmid DNA (1 mg/ml) using jetPRIME<sup>®</sup> reagent (Polyplus) according to the manufacturer's protocol was performed 24 h after seeding. Half of the coverslips were fixed with 2% PFA/0.075% GA in 1 $\times$  PBS and the other half with 4% PFA in PBS 24 h after transfection for 10 min. Each well with coverslip was washed three times with 1 $\times$  PBS (Sigma) for 10 min and mounted on microscope slides with Aqua PolyMount (PolyMount Sciences, Inc.) and kept at 4 $^{\circ}$ C after drying overnight.

## Ex utero electroporation

A mix of endotoxin-free plasmid preparation (2 mg/ml) and 0.5% Fast Green (Sigma) mixture was injected using FemtoJet 4i (Eppendorf) into the lateral ventricles of isolated heads of E15.5 mouse embryos. Embryonic neural progenitor cells were electroporated using an electroporator (ECM 830, BTX) and gold paddles with four pulses of 20 V for 50 ms with a 500 ms interval and an electrode gap of 1.0 mm. Dissociated primary neuron culture was performed after *ex utero* electroporation (EUE).

## Primary neuronal culture

Following EUE, embryonic mouse cortices (E15.5) were dissected in Hank's Balanced Salt Solution (HBSS) supplemented with HEPES (10 mM, pH 7.4) and incubated in HBSS containing papain (Worthington; 14 U/ml) and DNase I (100  $\mu$ g/ml) for 15 min at 37 $^{\circ}$ C with a gentle flick between incubation. Samples were washed with HBSS three times and dissociated by pipetting on the fourth wash. Cells were counted using Countess<sup>™</sup> (Invitrogen) and cell suspension was plated on poly-D-lysine (1 mg/ml, Sigma)-coated glass bottom dishes

(MatTek) or poly-D-lysine/laminin coated coverslips (BD bioscience) in Neurobasal media (Gibco) containing FBS (2.5%) (Sigma), B27 (1 $\times$ ) (Gibco), and Glutamax (1 $\times$ ) (Gibco). After 7 days, the media was changed with supplemented Neurobasal media without FBS.

## Fixation for primary neuron culture

Half of the culture dishes were fixed with 2% PFA (PFA Alfa Aesar)/0.075% GA (Electron Microscopy Science, EMS) in 1 $\times$  PBS (Sigma) and the other half was fixed with 4% PFA for 10 min. Dishes were washed three times following fixation with 1 $\times$  PBS (Sigma) for 10 min.

## In utero electroporation

A mix of endotoxin-free plasmid preparation (0.5 mg/ml) and 0.5% Fast Green (Sigma) was injected into one lateral hemisphere of E15.5 embryos using FemtoJet 4i (Eppendorf). Embryonic neural progenitor cells were labeled using the electroporator (ECM 830, BTX) with gold paddles at E15.5. Electroporation was performed by placing the anode (positively charged electrode) on the side of the DNA injection and the cathode on the other side of the head. Five pulses of 38 V for 50 ms with a 500 ms interval and an electrode gap of 1.0 mm were used for electroporation.

## Intracardial perfusion

For direct and indirect perfusion experiments in Figure 2, animals were put to sleep using 5% isoflurane mixed with air and exsanguinated 21 days after birth (P21) by terminal intracardial perfusion. Pups were randomly divided into four groups to test different perfusion conditions. 1 $\times$  PBS and fixatives were kept on ice during the entire procedure. Group 1 (indirect PFA/GA) was perfused with 10 ml of 1 $\times$  PBS followed by 30 ml of fixative 2% PFA/0.075% GA in PBS [diluted in 1 $\times$  PBS (Sigma) from 32% PFA (Alfa Aesar), and 3% GA (Electron Microscopy Science)]. Group 2 (indirect PFA) with 10 ml of PBS followed by 30 ml of 4% PFA in PBS. Group 3 (direct PFA/GA) by 30 ml of fixative 2% PFA/0.075% GA in PBS. Group 4 (direct PFA) 30 ml of 4% PFA in PBS. Animals were then dissected to isolate brains that were later subjected to 20 h post-fixation in the same fixative that was used for perfusion in each group.

For oxygen supplement-related experiments in Figure 3, mice were randomly assigned to anesthetize either with 2.5 vol% isoflurane with 2 ml/min oxygen or with isoflurane only. For the group with oxygen inhalation, isoflurane was delivered with oxygen through an anesthesia machine. A closed jar containing 1 ml of isoflurane was used to anesthetize the group

without oxygen. Mice were perfused transcardially with 2% PFA (Alfa Aesar) and 0.075% GA (Sigma) in PBS, and brains were isolated for further experiments. During the perfusion, pulse and oxygen concentration were measured with MouseSTAT<sup>®</sup> Jr. Pulse Oximeter and Heart Rate Monitor (Kent Scientific). After 2 h of post-fixation in the same fixative used in perfusion, brains were washed with PBS and sectioned using a vibratome (Leica VT1200) at 130  $\mu$ m. Sections were then washed three times with PBS and mounted on slides with VECTASHIELD<sup>®</sup> Vibrance<sup>™</sup> Antifade Mounting Medium with DAPI (Vector Laboratories).

## Imaging of cultured NIH3T3 cells and cultured neurons

Cultured cells were imaged on a Nikon Ti2 widefield system equipped with a Hamamatsu Fusion CMOS camera, standard cubes for FITC, TRITC, and DAPI, and 60 $\times$  (1.2 NA) oil objective, and a live imaging chamber from OXO. The whole system is controlled by Nikon Elements. For cultured NIH3T3 cells, cells were fixed as above and then imaged directly after fixation. For cultured neurons, cells were imaged live first and then fixed as above, and then the same cell was reimaged following fixation.

## Live imaging under hypoxic conditions

Live cell imaging under hypoxic conditions was performed with the EVOS M7000 imaging system (Thermo Scientific) equipped with an onstage incubator. A normal Tyrode solution was used as a bath solution, and neurons were incubated in a humidified atmosphere containing 5% CO<sub>2</sub> at 37°C. To induce the hypoxic condition, oxygen level was gradually decreased from 20 to 10%, then 10% to 5%, then 5% to 0.1%. Samples were imaged for 10 min with a 1 min interval in each oxygen level. One image per oxygen level was used to analyze the dendritic mitochondrial length in each condition.

## Imaging brain sections

For direct and indirect perfusion experiments in **Figure 2**, fixed samples were imaged on a Zeiss LSM 880 confocal microscope controlled by Zeiss Black software. Imaging required two lasers 488 and 561 nm together with Zeiss objectives 40 $\times$  (1.2 NA) with 2 $\times$  zoom, or 100 $\times$  oil (1.25 NA) with 3 $\times$  zoom.

For oxygen supplement-related experiments in **Figure 3**, fixed samples were imaged on a Nikon A1R confocal microscope with a Nikon objective 60 $\times$  (1.25 NA). Samples were visualized by Z-stacking that was later processed into Maximum Intensity Projection (MIP). MIP 2D images were then used for analysis

of mitochondrial length and occupancy using NIS Elements software (Nikon) and Fiji (ImageJ).

## $\alpha$ -Synuclein treatment

Active human recombinant  $\alpha$ -synuclein preformed fibrils (PFF) were purchased from StreeMarq. Before the treatment,  $\alpha$ -synuclein PFF was diluted in PBS at 0.1 mg/ml and sonicated for 30 s.  $\alpha$ -Synuclein was added at 10 DIV at a concentration of 1  $\mu$ g/ml and incubated for 11 days.

## Immunohistochemistry

Following fixation and washing, brains were embedded in 3% low melt agarose (RPI, A20070) in 1 $\times$  PBS. Brains in agarose cubes were sectioned using a vibratome (Leica VT1200) at 120  $\mu$ m. Sections were then incubated with primary antibodies (chicken anti-GFP Aves Lab 1:1,000, rabbit anti-dsRed Abcam 1:1,000) that were diluted in the blocking buffer (1% BSA, 0.2% Triton X-100, and 5% NGS in PBS) at 4°C for 48 h. Subsequently, sections were washed 6 times for 10 min in PBS and incubated with secondary antibodies (Alexa conjugated goat anti-chicken 488 and goat anti-rabbit 568 1:1,000) at 4°C for 48 h. The excess of secondary antibodies was removed by six, 10 min washes in 1 $\times$  PBS. Sections were then mounted on slides and coverslipped with Aqua PolyMount (PolyMount Sciences, Inc.) and kept at 4°C.

## Immunocytochemistry

Cultured neurons were fixed for 15 min at room temperature in either 4% PFA, 2% PFA with 0.075% GA, or 4% PFA with 4% sucrose and then washed with PBS. The cells were permeabilized with 0.2% Triton X-100 in PBS and incubation in 0.1% BSA and 2.5% goat serum in PBS was followed to block non-specific signals. Primary and secondary antibodies were diluted in the blocking buffer described above and incubated at 4°C overnight. Coverslips were mounted on slides with VECTASHIELD<sup>®</sup> Vibrance<sup>™</sup> Antifade Mounting Medium (Vector Laboratories). Primary antibodies used in this experiment were mouse anti-HA (Biolegend, 1:500) and rabbit anti- $\alpha$ -synuclein (pS129) (Abcam, 1:300), and all secondary antibodies were Alexa-conjugated (Invitrogen) and used at a 1:1,000 dilution.

## Quantification and statistical analysis

For the data in **Figures 1, 2**, individual mitochondria were measured *via* the matrix-targeted yellow fluorescent protein

(mt-YFP) signal from isolated, secondary dendrite segments with NIS Elements AR (Nikon) using the length measurement tool on the raw images. For data in **Supplementary Figure 1**, individual cells were selected in Fiji (ImageJ – NIH), the mt-YFP signal was then isolated, and subtract background was run with a 10 px ball. This image was then run through the Enhance local contrast [63 block, 2.0 slope, Autocontrast (IsoData)] and Despeckle commands. Finally, the lookup table was inverted, and the image was analyzed with Analyze particles (0.06-Infinity). For the data in **Figures 3–5**, individual mitochondria from isolated secondary dendrite segments were measured in Fiji using the measurement tool for length on the raw images. Cumulative frequency graphs were created by plotting all mitochondria measured for length along the *x*-axis vs. their frequency within the total population along the *y*-axis. Mitochondria size distribution graphs show individual mitochondria lengths *via* the symbols with the mean plus error listed in each figure legend.

Statistical analysis was done in GraphPad's Prism 6. Statistical tests, *p*-values, and (*n*) numbers are presented in the figure legends. The Gaussian distribution was tested using D'Agostino and Pearson's omnibus normality test. We applied non-parametric tests when data from groups tested deviated significantly from normality. No blinding was performed. No sample size calculation was performed. No exclusion criteria were pre-determined and no animals were excluded. All analyses were performed on raw imaging data without any adjustments. Images in the figures have been adjusted for brightness and contrast (identical for control and experimental conditions in groups compared), and images in **Figure 2** have been processed with Nikon's proprietary denoise.ai for visualization purposes only.

## Results

### Fixation of cultured cells with a solution of paraformaldehyde/glutaraldehyde better preserves mitochondrial morphology

Based on our own observations and the high variation that has been reported in the literature for mitochondrial morphology in neurons, we hypothesized that standard fixation conditions with 4% PFA may not be optimal for maintaining mitochondrial structure. To test this hypothesis, we performed EUE coupled with primary neuron culture to visualize mitochondrial morphology at single cell resolution in culture. Following culture for 17 days to allow for neuronal maturation, we first imaged neurons live at 37°C [**Figure 1A** (top)], followed by immediate fixation with a 4% PFA solution in PBS and

three PBS washes on the stage, allowing us to image the same neurons following fixation [**Figure 1A** (bottom)]. As published previously by multiple groups, dendritic mitochondria are highly elongated and tubular in cortical PNs (Popov et al., 2005; Chang and Reynolds, 2006; Lewis et al., 2018; Rangaraju et al., 2019) and occupy a large portion of the dendritic arbor in living neurons. However, upon fixation with 4% PFA, we observed a rapid fragmentation of dendritic mitochondria, leading to smaller mitochondria (live dendritic mitochondria mean length:  $4.9 \pm 0.27 \mu\text{m}$ ; after 4% PFA fixation:  $2.3 \pm 0.14 \mu\text{m}$ ). This result confirmed that fixation with only a solution of 4% PFA is not optimal for maintaining the mitochondrial morphology observed in living neurons. To determine a perfusion solution that would better preserve mitochondrial morphology during fixation, we searched the literature and observed that many groups performing EM included GA in their fixation solution as it provides increased cross-linking activity compared to PFA alone. To test if a solution of PFA/GA would achieve more optimal preservation of mitochondrial morphology, we performed the same experiment as above but used a fixative solution of 2% PFA/0.075% GA to fix the cultured neurons (**Figure 1B**). As clearly observed and quantified (**Figures 1C,D**), a solution of 2% PFA/0.075% GA dramatically reduced mitochondrial fragmentation during fixation (live dendritic mitochondria mean length:  $5.2 \pm 0.29 \mu\text{m}$ ; after PFA/GA:  $4.2 \pm 0.23 \mu\text{m}$ ). Finally, we asked if this was a result specific to the fixation of neuronal mitochondria or if it would be conserved in other cell types. Using cultured NIH3T3 cells transfected to fluorescently labeled mitochondria, we compared fixation with either 4% PFA or a solution of 2% PFA/0.075% GA (**Supplementary Figure 1**). We observed very similar results to neurons with 4% PFA, leading to a decrease in total mitochondrial area (4% PFA:  $105.3 \mu\text{m}^2$  vs.  $188.4 \mu\text{m}^2$  for 2% PFA/0.075% GA) and increased circularity (4% PFA:  $0.78 \pm 0.01$  vs.  $0.58 \pm 0.01$  for 2% PFA/0.075% GA).

### Direct perfusion results in the consistent preservation of mitochondrial morphology

Following this observation in cultured neurons, we tested if it applies to the preservation of mitochondrial morphology in neurons *in vivo*. To test this, we performed IUE on E15.5 CD1 pups with a plasmid encoding a mitochondrial mt-YFP. At (P)ostnatal day 21, when several aspects of neuronal differentiation, including dendritic morphogenesis and synaptogenesis, are adult-like, mice were anesthetized with isoflurane and intracardiac perfusion was performed. Initial attempts resulted in a significant degree of mitochondrial fragmentation or loss of elongated mitochondria in perfused brains regardless of fixation solution (**Figures 2A,B,E,F**). We then tested various buffers, buffer pH and buffer temperatures,



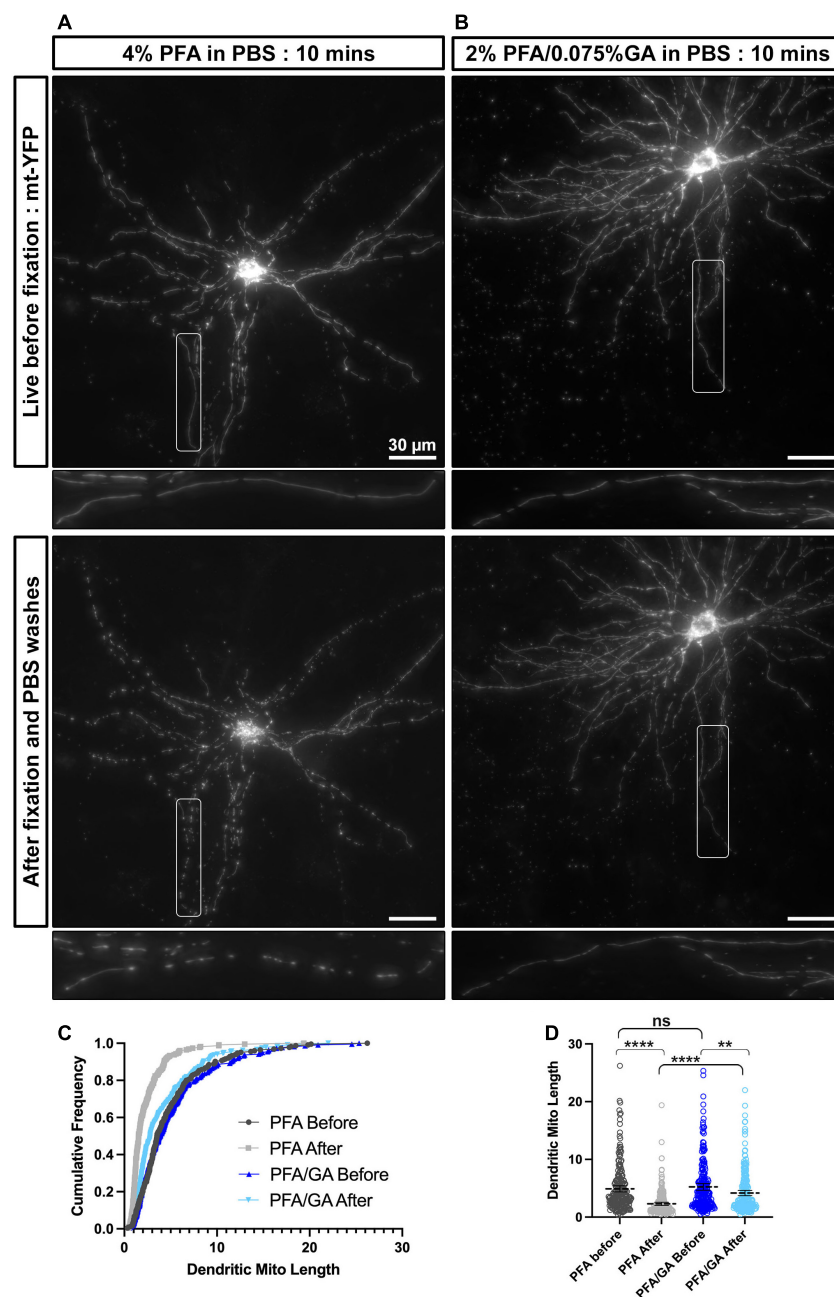


FIGURE 1

A combination of PFA and GA maintains mitochondria morphology better than PFA alone in cultured cortical neurons. **(A)** A representative neuron labeled with mitochondrial matrix targeted YFP (mt-YFP) imaged live before fixation (**top**) and after fixation with 4% PFA in PBS (**bottom**). **(B)** A representative neuron labeled with mt-YFP imaged live before fixation (**top**) and after fixation with 2% PFA/0.075% GA in PBS (**bottom**). **(C)** Cumulative frequencies of dendritic mitochondrial length showing that fixation with PFA only results in fragmentation of mitochondria. **(D)** Quantification of dendritic mitochondrial lengths shown as mean  $\pm$  95% CI before and after fixation with the indicated fixative solution. Kruskal–Wallis test with Dunn’s multiple comparisons test.  $n_{4\%PFA\text{before}} = 2$  cultures, 16 dendrites, 225 mitochondria,  $n_{4\%PFA\text{after}} = 2$  cultures, 16 dendrites, 227 mitochondria,  $n_{PFA/GA\text{before}} = 2$  cultures, 16 dendrites, 222 mitochondria, and  $n_{PFA/GA\text{after}} = 2$  cultures, 16 dendrites, 238 mitochondria. \*\* $p < 0.01$ , \*\*\* $p < 0.001$ , \*\*\*\* $p < 0.0001$ . Scale bar, 30  $\mu\text{m}$ .

but none preserved the elongated mitochondria observed in the dendrites (data not shown). Finally, we attempted direct perfusion where instead of performing a pre-flush with PBS or other buffers to remove blood, we directly started the perfusion

with the fixative solution. Strikingly, this resulted in consistent preservation of the elongated mitochondria morphology observed in living neuronal dendrites (**Figures 2C–F**). While PFA/GA still resulted in the most elongated mitochondrial

network, even with PFA 4% alone, direct perfusion led to a more consistent preservation of mitochondria morphology *in vivo* (dendritic mitochondria mean length: indirect PFA –  $1.95 \pm 0.1 \mu\text{m}$ , direct PFA –  $4.5 \pm 0.4 \mu\text{m}$ , indirect PFA/GA –  $1.5 \pm 0.1 \mu\text{m}$ , direct PFA/GA –  $5.4 \pm 0.5 \mu\text{m}$ ), and is clearly a critical step in capturing the *in vivo* structure of mitochondria.

## Anesthesia without oxygen supply during perfusion induces mitochondrial fragmentation

We confirmed that direct perfusion could preserve mitochondrial morphology during perfusion. However, variance in dendritic mitochondrial length is still observed in previous studies and in our experiments while using direct perfusion and suggested that there is another important factor affecting mitochondrial morphology. Because oxygen levels in mice may change depending on the oxygen supply during anesthesia, and it has been reported that oxygen deprivation can induce mitochondrial fragmentation in several cell types, we examined if anesthesia with and without oxygen supply would result in differences in mitochondrial morphology. In order to study mitochondrial morphology after perfusion, we sparsely labeled mouse PNs using IUE with a Cre-dependent plasmid containing a mitochondria-targeted fluorescent protein and a low concentration of a Cre recombinase-expressing plasmid (**Supplementary Figure 2**). At P21, mice were anesthetized either with an anesthesia machine, which delivers isoflurane with oxygen, or with a closed jar containing isoflurane and directly perfused with 2% PFA/0.075% GA. Oxygen concentration and pulse rate were monitored with a pulse oximeter during perfusion. Anesthesia without oxygen supplement showed significantly decreased oxygen concentration ( $86.78\% \pm 1.00\%$  with oxygen vs.  $55.68\% \pm 1.93\%$  without oxygen) and increased pulse rate compared to with oxygen ( $337.1 \pm 5.89$  pulses/min with oxygen vs.  $459.5 \pm 3.36$  pulses/min without oxygen, **Figures 3D,E**). Next, we compared the length of dendritic mitochondria in each condition. Strikingly, mice anesthetized without oxygen showed significantly shortened dendritic mitochondria after perfusion ( $2.30 \pm 0.20 \mu\text{m}$  without oxygen vs.  $6.74 \pm 0.51 \mu\text{m}$  with oxygen, **Figures 3A–C**). These results suggest that avoidance of hypoxic condition is critical for preserving the mitochondrial morphology of neurons *in vivo*.

## Reduced oxygen level causes changes of mitochondrial morphology *in vitro*

To ascertain what level of hypoxia can result in mitochondrial fragmentation, we next tested if gradual changes in oxygen level could directly affect mitochondrial morphology.

Live imaging of fluorescently mitochondria-labeled cortical neurons *in vitro* allowed us to observe changes in mitochondrial morphology in real time. We incubated neurons under normoxic (20% oxygen) and hypoxic conditions (10, 5, 0.1% oxygen). As oxygen level dropped, the length of dendritic mitochondria gradually decreased (from  $10.21 \pm 0.64 \mu\text{m}$  in 20% oxygen to  $6.96 \pm 0.46 \mu\text{m}$  in 0.1% oxygen, **Figure 4**). Coupled with our previous *in vivo* perfusion observations, these results emphasize the importance of oxygen concentration for maintaining mitochondrial morphology during fixation.

## Fixation protocol affects the outcome of mitochondrial analysis in neurodegenerative disease models

Mitochondrial dysfunction is a hallmark of neurodegeneration. Fragmentation of dendritic mitochondria is observed in many neurodegenerative diseases, including Alzheimer's disease and Parkinson's diseases (Wang et al., 2009; Matheoud et al., 2016; Zhang et al., 2016; Burbulla et al., 2017; Lee et al., 2018). As shown in **Figures 1, 2**, fixation with 4% PFA resulted in fragmentation of mitochondria, while 2% PFA with 0.075% GA showed intact morphology. Because different compositions of fixative could alter mitochondrial morphology, we assumed that this could influence the analysis of mitochondria in models of neurodegenerative disease. To test this, we investigated the effect of three different fixation solutions using an  $\alpha$ -synuclein preformed fibril (PFF)-induced synucleinopathy model. Neurons were incubated with  $\alpha$ -synuclein for 11 days starting from 10 DIV and then fixed with three different fixatives; 4% PFA, 2% PFA with 0.075% GA, or 4% PFA with 4% sucrose.  $\alpha$ -Synuclein fibril accumulation was confirmed with phosphorylated  $\alpha$ -synuclein staining, which is a marker for accumulated  $\alpha$ -synuclein in cells (**Supplementary Figure 3**). To determine if the fixation solution could affect the analysis outcome of mitochondrial morphology, we compared the differences in dendritic mitochondrial length between control and  $\alpha$ -synuclein treated samples in each fixation condition. With 2% PFA/0.075% GA, control mitochondrial morphology was consistent with the results presented above, while  $\alpha$ -synuclein treated samples showed a significant decrease in average dendritic mitochondrial length ( $2.80 \pm 0.09$  vs.  $3.35 \pm 0.13 \mu\text{m}$  in control, **Figure 5**). However, fixation with only 4% PFA abolished the differences observed in dendritic mitochondrial length following  $\alpha$ -synuclein treatment ( $2.26 \pm 0.07$  vs.  $2.17 \pm 0.06 \mu\text{m}$  in control, **Figure 5**) as control mitochondria were much shorter than with PFA/GA. Although PFA/GA fixation was ideal for preserving mitochondrial morphology, there are high background autofluorescence signals following immunocytochemistry. Thus, we also tested 4% PFA/4% sucrose as an alternative solution, which is known to be cryoprotective. Compared with PFA only, PFA with

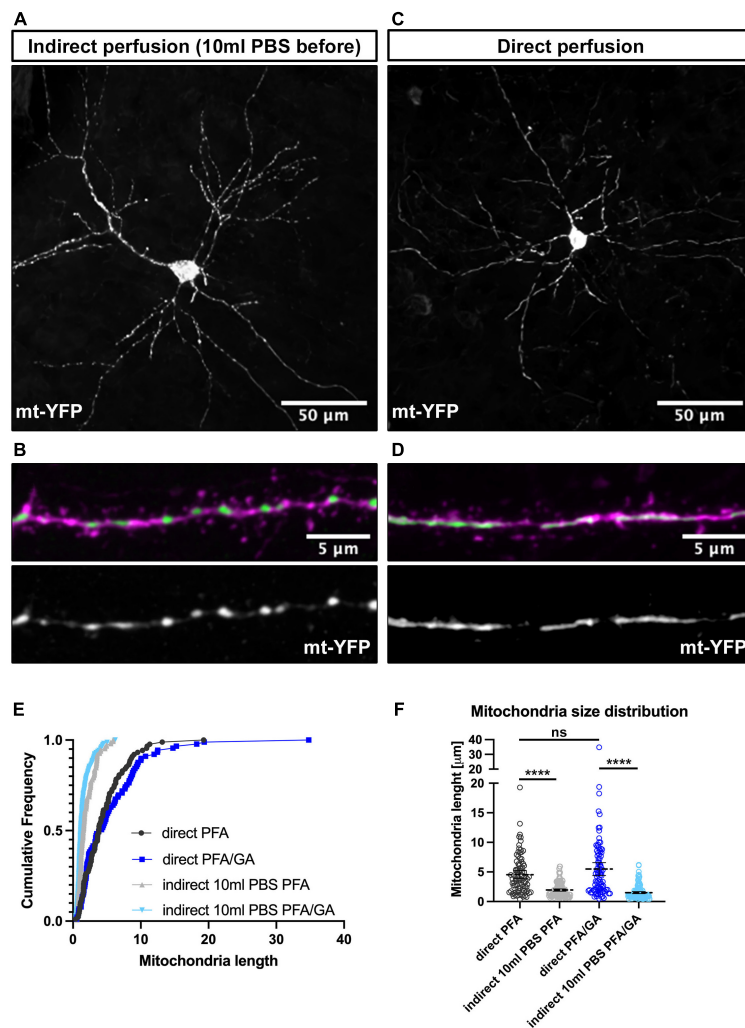


FIGURE 2

Direct perfusion is necessary for preserving mitochondrial morphology *in vivo*. (A) Low magnification representative neuron following indirect perfusion with PFA/GA solution. (B) High magnification of a dendrite segment following indirect perfusion with PFA/GA. (C) Low magnification representative neuron following direct perfusion with PFA/GA solution. (D) High magnification of a dendrite segment following direct perfusion with PFA/GA. (E) Cumulative frequencies of dendritic mitochondrial length showing that indirect perfusion results in fragmentation of mitochondria. (F) Quantification of dendritic mitochondrial lengths shown as mean  $\pm$  95% CI before and after fixation with the indicated fixative solution. Kruskal–Wallis test with Dunn’s multiple comparisons test.  $n_{\text{indirectPFA}} = 15$  dendrites, 150 mitochondria,  $n_{\text{directPFA}} = 11$  dendrites, 88 mitochondria,  $n_{\text{indirectPFA/GA}} = 13$  dendrites, 158 mitochondria, and  $n_{\text{directPFA/GA}} = 14$  dendrites, 88 mitochondria. ns, not significant, \*\*\*\* $p < 0.0001$ . Scale bar, 50  $\mu\text{m}$  for A,C, 5  $\mu\text{m}$  for B,D.

sucrose preserved mitochondrial morphology closer to PFA/GA fixation but with lower background signals (Figure 5B and Supplementary Figure 3). Overall, these results suggest that fixation solutions will affect the results of mitochondrial morphology analysis and that this parameter should be carefully weighed during the experimental design phase.

## Discussion

Our results clearly demonstrate that the method of fixation is critical for preserving the mitochondria morphology

observed in living mammalian neurons. Our findings can be broken down into three main observations: (1) direct fixation is critical both in cultured neurons and *in vivo*. Any condition which included significant pre-washing with PBS or other saline solutions to remove culture medium or blood resulted in fragmentation of the mitochondria. (2) Preventing hypoxia is required to maintain mitochondrial structure. Conditions that resulted in low oxygen were sufficient to induce mitochondrial fragmentation both *in vitro* and *in vivo*. (3) A mixture of PFA/GA most faithfully preserved the mitochondrial morphologies and sizes observed in living neurons. This appears especially true with cultured neurons, as even direct fixation



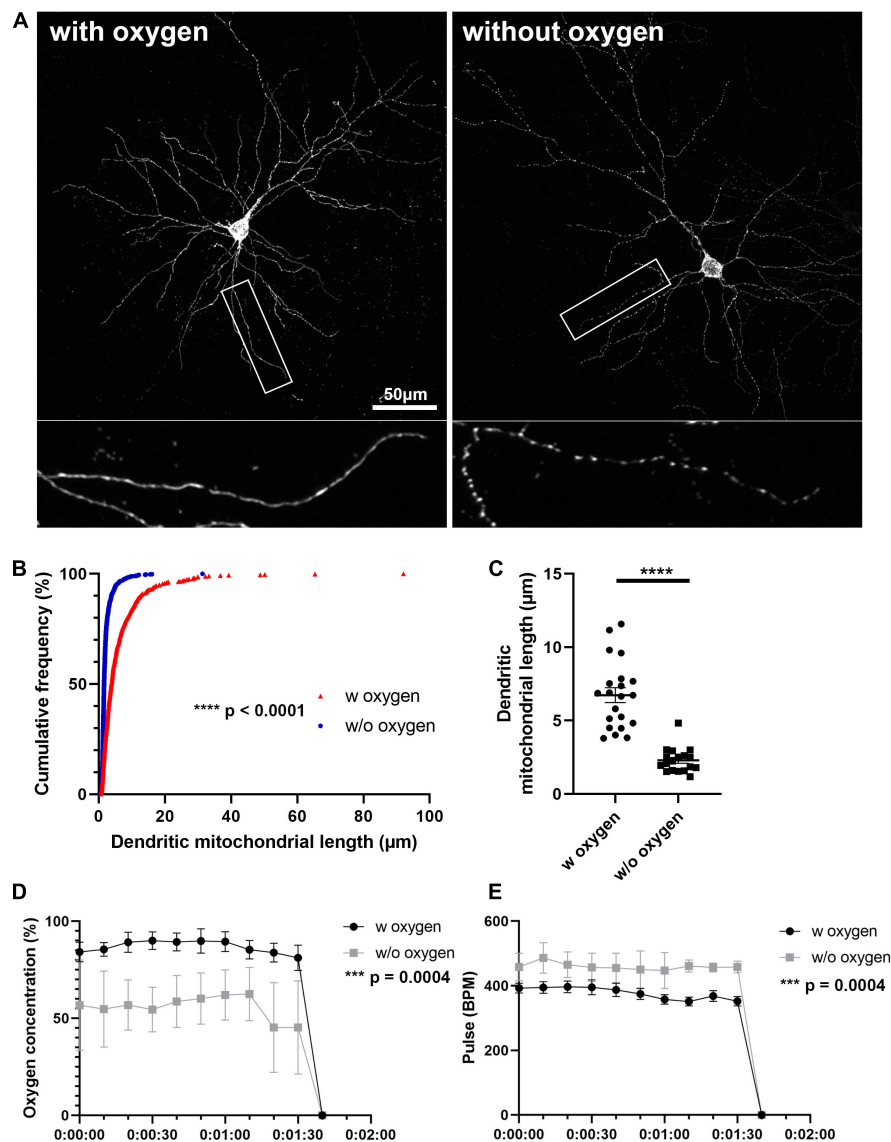


FIGURE 3

Oxygen supply is necessary for preserving mitochondrial morphology during anesthesia and perfusion. (A) Representative images of mitochondria after perfusion. (B) Cumulative frequencies of dendritic mitochondrial length showing that perfusion without oxygen supplement results in fragmentation of mitochondria.  $n_{\text{with oxygen}} = 627$  mitochondria and  $n_{\text{without oxygen}} = 1061$  mitochondria. Kolmogorov–Smirnov test, \*\*\*\* $p < 0.001$ . (C) Quantification of dendritic mitochondria in each perfusion condition confirmed shorter mitochondria in perfusion without oxygen compared to perfusion with oxygen.  $n_{\text{with oxygen}} = 42$  dendrites and  $n_{\text{without oxygen}} = 36$  dendrites. Unpaired  $t$ -test, \*\*\*\* $p < 0.0001$ . (D,E) Oxygen concentration and pulse were measured during perfusion procedure.  $n_{\text{with oxygen}} = 7$  mice and  $n_{\text{without oxygen}} = 6$  mice. Mann–Whitney test, \*\*\* $p = 0.0004$ . Scale bar, 50  $\mu\text{m}$ .

with 4% PFA resulted in fragmented mitochondria. However, *in vivo*, if conditions one and two are met, we observed only a small decrease in mitochondrial length with 4% PFA compared to 2% PFA/0.075% GA (Supplementary Table 1). Together, our results establish that it is critical for the fixation process to occur as rapidly as possible in order to maintain the mitochondria structure observed in living neurons, and if this is not carefully considered, the fixative conditions may result in incorrect conclusions, as we have shown with  $\alpha$ -synuclein treatment.

Surprisingly, “standard” published protocols for the perfusion of rodents and other small animals show considerable variability (Gage et al., 2012; Uhlig et al., 2015; Wu et al., 2021; Buffalo, 2022; Montana, 2022). This variability mainly comes in many forms: the anesthesia used to prepare the animal for the procedure, the buffers and/or fixatives used during the procedure, and the length of time the fixation solution stays in contact with the sample of interest. The choices made at each of these steps will have important ramifications on the

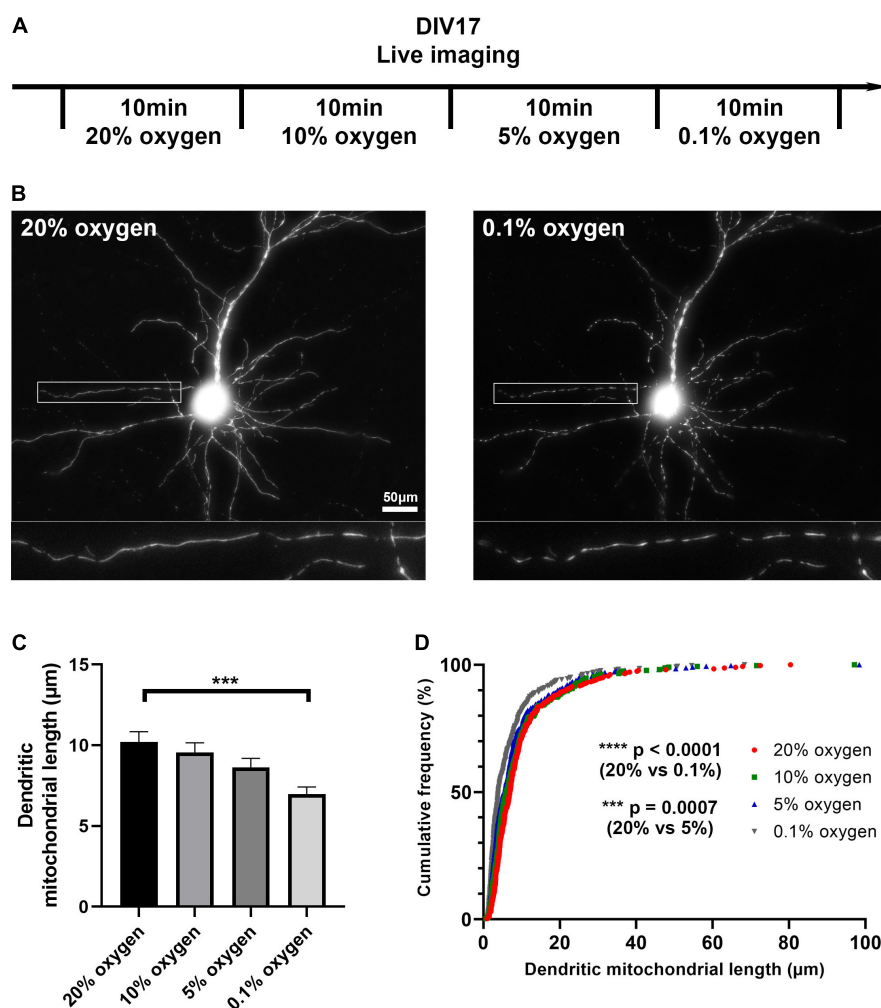


FIGURE 4

Low oxygen level induces mitochondrial fragmentation *in vitro*. (A) Schematic diagram of live imaging. Live imaging of mitochondria-labeled cortical neurons was done in four different oxygen levels; 20, 10, 5, and 0.1%. (B) Representative images of mitochondria in 20 and 0.1% oxygen level. (C) Quantification of dendritic mitochondrial length showed gradual decrease as oxygen level dropped. (D) Cumulative frequencies of dendritic mitochondrial length also showed shorter mitochondria in low oxygen level, compared to normal oxygen level.  $n_{20\% \text{ oxygen}} = 2$  cultures, 26 dendrites, 316 mitochondria,  $n_{10\% \text{ oxygen}} = 2$  cultures, 26 dendrites, 323 mitochondria,  $n_{5\% \text{ oxygen}} = 2$  cultures, 26 dendrites, 330 mitochondria, and  $n_{0.1\% \text{ oxygen}} = 2$  cultures, 26 dendrites, 346 mitochondria. Kruskal–Wallis test with Dunn’s multiple comparisons test. Length: \*\*\* $p = 0.0007$  for 20% oxygen vs. 5% oxygen, \*\*\*\* $p < 0.0001$  for 20% oxygen vs. 0.1% oxygen. Scale bar, 20 µm.

outcome of the procedure, and the decision should depend on the ultimate focus of the investigator. For instance, in our hands, overall neuronal cell structure (i.e., dendrites, axons, and spines) appeared to be well preserved with all the anesthetics and fixatives we tested, even though mitochondrial structure showed the striking differences detailed above (data not shown). The length of time in the fixation solution was not carefully examined in our study, and thus is a potential limitation of the current study.

While future work is still required to fully understand the mechanism, we found that exposing mitochondria to a short-term hypoxic environment is sufficient to induce mitochondrial fragmentation. Molecularly, this could be through mTOR-Drp1

mediated activation or by increased FUNDC1-Drp1 interaction (Wu et al., 2016; Zheng et al., 2019). Interestingly, *in vivo* hypoxic conditions triggered more significant mitochondrial fragmentation (less than 2 min) than in cultured neurons, which might be caused by the fast delivery of low-oxygen blood and/or solutions. Both the mode of anesthesia and the mode of perfusion likely play a role in the induction of this hypoxic state. Our results argue that when studying mitochondria, methods of anesthesia resulting in low oxygen levels should be avoided (i.e., CO<sub>2</sub> and drop isoflurane). Recent work demonstrates that oxygen supplementation is required to prevent hypoxia with both inhaled and injected anesthetics (Blevins et al., 2021). One step that is preserved across most published

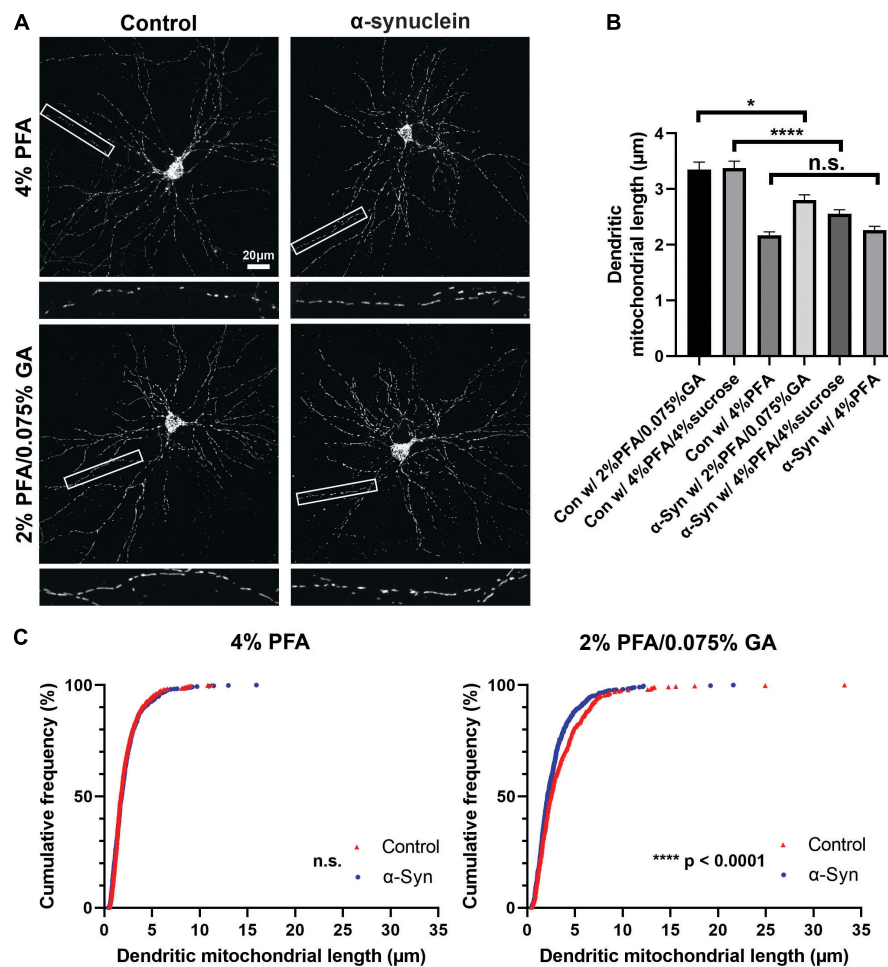


FIGURE 5

Fixative affects mitochondrial morphology analysis of a neurodegenerative disease model. (A) Images of control and  $\alpha$ -synuclein-treated neurons, which were fixed with three different fixation solutions (4% PFA, 2% PFA/0.075% GA, and 4% PFA/4% sucrose) for 15 min at DIV21. (B) Quantification of dendritic mitochondrial length confirmed 2% PFA/0.075% GA and 4% PFA/4% sucrose fixed samples showed differences between  $\alpha$ -synuclein-treated neurons and control neurons. In contrast, there were no differences in 4% PFA fixed samples.  $n_{\text{Con w/4\%PFA}} = 3$  cultures, 34 dendrites, 510 mitochondria,  $n_{\text{Con w/PFA/GA}} = 3$  cultures, 32 dendrites, 442 mitochondria,  $n_{\text{Con w/PFA/sucrose}} = 3$  cultures, 32 dendrites, 625 mitochondria,  $n_{\alpha\text{-syn w/4\%PFA}} = 3$  cultures, 32 dendrites, 587 mitochondria,  $n_{\alpha\text{-syn w/PFA/GA}} = 3$  cultures, 34 dendrites, 642 mitochondria, and  $n_{\alpha\text{-syn w/PFA/sucrose}} = 3$  cultures, 36 dendrites, 629 mitochondria. Kruskal–Wallis test with Dunn’s multiple comparisons test,  $*p = 0.03$  for control vs.  $\alpha$ -syn in 2% PFA/0.075% GA,  $****p < 0.0001$  for control vs.  $\alpha$ -syn in 4% PFA/4% sucrose. (C) Cumulative frequencies of dendritic mitochondrial length in 4% PFA showing no differences in dendritic mitochondria. (D) Cumulative frequencies of dendritic mitochondrial length in 2% PFA/0.075% GA fixation.

perfusion protocols is a saline-based flush (Gage et al., 2012; Wu et al., 2021; Buffalo, 2022; Montana, 2022). While this step removes blood, it likely exacerbates the hypoxia in the sample and should clearly be avoided when downstream analysis of mitochondria morphology will be performed. While not tested directly, antidotally, we did not observe any mitochondrial fragmentation in cultured neurons with a single quick rinse (less than 1 min) with PBS.

Two recent papers (Qin et al., 2021; Hinton et al., 2022) have independently come to some of the same conclusions about the role of fixation on mitochondria structure; nonetheless, key differences exist between in our findings. Hinton et al. used

EM to show that anesthesia with an isoflurane/oxygen mixture provided better preservation of mitochondrial structure than  $\text{CO}_2$ -based methods. In addition, direct perfusion of 4% PFA compared to PBS flushing conditions after injectable anesthesia (ketamine/xylazine) maintained mitochondrial shape. However, both the oxygen supplement and direct perfusion method were followed by strong fixative (Trump’s solution; 4% formaldehyde/1% GA) immersion, and the actual oxygen level was not monitored. Our study combined the oxygen supplementation and direct perfusion of fixative, and checked and manipulated the oxygen level *in vivo* and *in vitro*. Therefore, we could unambiguously conclude that the hypoxic condition

caused the fragmentation of mitochondria. While Qin et al. show that PFA/GA mixtures preserve mitochondria structure better *via* fluorescence imaging, much higher concentrations of GA were tested (2.5–1.5%) and the experiments were performed in MEFs, not neurons. High concentrations of GA cause strong background signals during immunocytochemistry, thus we find that the combination of low GA concentration coupled with the oxygenated/direct perfusion allows for both the preservation of mitochondria structure and for immunocytochemistry in the same brain samples.

Our results also argue that we should carefully consider the role that the method of fixation may have played in findings about mitochondrial morphology or structure. This may impact the outcome in a few different ways. One situation would be an incorrect negative result where incorrect perfusion leads to all conditions giving rise to similarly highly fragmented mitochondria as a result of a slow fixation process (Figure 5). In another situation, sub-optimal fixation conditions could give rise to a false positive result. For instance, under a pathogenic situation, stressed mitochondria could be structurally similar in the living cells but are more sensitive to the fixation process, leading to fixation-induced fragmentation only in the stressed mitochondria. Clearly, the gold standard would be to visualize mitochondrial structure under living conditions, which would remove the potential for fixation artifacts.

A potential confounding factor in the variation observed in the literature regarding mitochondrial length is recent data reporting differential mitochondria morphologies in different brain regions. It is now clear that both distinct neuron types and even the compartments within the same neuron (soma, dendrites, and axon) regulate mitochondria morphology to different levels (Faits et al., 2016; Lewis et al., 2018; Chandra et al., 2019; Janickova et al., 2020; Fajt et al., 2021; Lee et al., 2022). However, it is unclear if or how these different mitochondrial populations would be affected by the different fixatives and perfusion methods.

In each condition that we tested, a fixative solution of PFA/GA maintained mitochondrial morphology closer to those observed in living neurons. However, fixing with PFA/GA does have potential drawbacks that may limit its usefulness based on the context of the experiment. First, PFA/GA fixation causes increased background fluorescence across the visible wavelengths. Therefore, if trying to visualize a lowly expressed protein, the high background may reduce the signal-to-noise ratio to a level that is unacceptable. With regard to antibody staining, incubation times need to be significantly increased presumably because of the increased crosslinking that occurs with the PFA/GA fixation. We routinely had to double our antibody incubation times for 100  $\mu$ m thick brain sections from 16–24 h with PFA only to 32–48 h following PFA/GA fixation. In addition, the use of a 4% PFA/4% sucrose fixative solution showed less background signal without affecting dendritic mitochondrial

length *in vitro* (Figure 5 and Supplementary Figure 3); therefore, this may also be considered for immunocytochemistry experiments.

Taken together, our results provide standard anesthesia and fixation methods for the study of neuronal mitochondrial morphology both *in vitro* and *in vivo*. These results can also serve as a starting point when investigating other cellular mechanisms that are vulnerable to environmental stress.

## Data availability statement

The original contributions presented in this study are included in the article/Supplementary material, further inquiries can be directed to the corresponding authors.

## Ethics statement

This animal study was reviewed and approved by the Institutional Animal Care and Use Committee – Oklahoma Medical Research Foundation and the Institutional Animal Care and Use Committee – Korea Institute of Science and Technology.

## Author contributions

S-KK and TL: conceptualization, funding acquisition, and resources. SYK, KS, BO, S-KK, and TL: formal analysis, investigation, methodology, and visualization. KH, S-KK, and TL: project administration and supervision. SYK, S-KK, and TL: writing—original draft. SYK, KS, BO, KH, S-KK, and TL: writing—review and editing. All authors contributed to the article and approved the submitted version.

## Funding

This research was supported by the National Research Foundation (NRF) funded by the Korean Government (MSIT) (2019M3E5D2A01063794, 2020R1C1C1006386, and 2022M3E5E8017395) and KIST Program (2E31511) to S-KK, and OMRF startup funds and support from the Presbyterian Health Foundation to TL.

## Acknowledgments

We thank Julien Courchet, Yusuke Hirabayashi, and Franck Polleux for discussions and critical feedback on the manuscript. We also thank all members of the Kwon and Lewis labs for feedback and discussion along the way.

## Conflict of interest

The authors declare that the research was conducted in the absence of any commercial or financial relationships that could be construed as a potential conflict of interest.

## Publisher's note

All claims expressed in this article are solely those of the authors and do not necessarily represent those of their affiliated organizations, or those of the publisher, the editors and the reviewers. Any product that may be evaluated in this article, or claim that may be made by its manufacturer, is not guaranteed or endorsed by the publisher.

## Supplementary material

The Supplementary Material for this article can be found online at: <https://www.frontiersin.org/articles/10.3389/fnmol.2022.1042616/full#supplementary-material>

## References

- Azzu, V., and Valencak, T. G. (2017). Energy metabolism and ageing in the mouse: A mini-review. *Gerontology* 63, 327–336. doi: 10.1159/000454924
- Belanger, M., Allaman, I., and Magistretti, P. J. (2011). Brain energy metabolism: Focus on astrocyte-neuron metabolic cooperation. *Cell Metab.* 14, 724–738. doi: 10.1016/j.cmet.2011.08.016
- Blevins, C. E., Celeste, N. A., and Marx, J. O. (2021). Effects of oxygen supplementation on injectable and inhalant anesthesia in C57BL/6 mice. *J. Am. Assoc. Lab. Anim. Sci.* 60, 289–297. doi: 10.30802/AALAS-JAALAS-20-000143
- Buffalo, U. O. (2022). *Standard operating procedures for whole body perfusion fixation of mice*. Available online at: [https://www.buffalo.edu/content/dam/www/research/pdf/laf/sop/2A12.pdf\\_\(accessed February 9, 2022\)](https://www.buffalo.edu/content/dam/www/research/pdf/laf/sop/2A12.pdf_(accessed February 9, 2022)).
- Burbulla, L. F., Song, P., Mazzulli, J. R., Zampese, E., Wong, Y. C., Jeon, S., et al. (2017). Dopamine oxidation mediates mitochondrial and lysosomal dysfunction in Parkinson's disease. *Science* 357, 1255–1261.
- Chandel, N. S. (2014). Mitochondria as signaling organelles. *BMC Biol.* 12:34. doi: 10.1186/1741-7007-12-34
- Chandra, R., Calarco, C. A., and Lobo, M. K. (2019). Differential mitochondrial morphology in ventral striatal projection neuron subtypes. *J. Neurosci. Res.* 97, 1579–1589. doi: 10.1002/jnr.24511
- Chang, D. T. W., and Reynolds, I. J. (2006). Differences in mitochondrial movement and morphology in young and mature primary cortical neurons in culture. *Neuroscience* 141, 727–736. doi: 10.1016/j.neuroscience.2006.01.034
- Diaz-Garcia, C. M., and Yellen, G. (2019). Neurons rely on glucose rather than astrocytic lactate during stimulation. *J. Neurosci. Res.* 97, 883–889. doi: 10.1002/jnr.24374
- Faitg, J., Laceyfield, C., Davey, T., White, K., Laws, R., Kosmidis, S., et al. (2021). 3D neuronal mitochondrial morphology in axons, dendrites, and somata of the aging mouse hippocampus. *Cell Rep.* 36:109509. doi: 10.1016/j.celrep.2021.109509
- Faits, M. C., Zhang, C., Soto, F., and Kerschensteiner, D. (2016). Dendritic mitochondria reach stable positions during circuit development. *Elife* 5:e11583. doi: 10.7554/eLife.11583
- Fox, P. T., Raichle, M. E., Mintun, M. A., and Dence, C. (1988). Nonoxidative glucose consumption during focal physiologic neural activity. *Science* 241, 462–464. doi: 10.1126/science.3260686
- Gage, G. J., Kipke, D. R., and Shain, W. (2012). Whole animal perfusion fixation for rodents. *J. Vis. Exp.* 30:3564. doi: 10.3791/3564
- Gonzalez-Rodriguez, P., Zampese, E., Stout, K. A., Guzman, J. N., Ilijic, E., Yang, B., et al. (2021). Disruption of mitochondrial complex I induces progressive parkinsonism. *Nature* 599, 650–656.
- Hinton, A., Katti, P., Christensen, T. A., Mungai, M., Shao, J., Zhang, L., et al. (2022). A comprehensive approach to artifact-free sample preparation and the assessment of mitochondrial morphology in tissue and cultured cells. *bioRxiv* [Preprint]. doi: 10.1101/2021.06.27.450055
- Janickova, L., Rechberger, K. F., Wey, L., and Schwaller, B. (2020). Absence of parvalbumin increases mitochondria volume and branching of dendrites in inhibitory PVALB neurons in vivo: A point of convergence of autism spectrum disorder (ASD) risk gene phenotypes. *Mol. Autism* 11:47. doi: 10.1186/s13229-020-00323-8
- Kimura, T., and Murakami, F. (2014). Evidence that dendritic mitochondria negatively regulate dendritic branching in pyramidal neurons in the neocortex. *J. Neurosci.* 34, 6938–6951. doi: 10.1523/JNEUROSCI.5095-13.2014
- Kwon, S. K., Sando, R. III, Lewis, T. L., Hirabayashi, Y., Maximov, A., and Polleux, F. (2016). LKB1 regulates mitochondria-dependent presynaptic calcium clearance and neurotransmitter release properties at excitatory synapses along cortical axons. *PLoS Biol.* 14:e1002516. doi: 10.1371/journal.pbio.1002516
- Lee, A., Hirabayashi, Y., Kwon, S. K., Lewis, T. L. Jr., and Polleux, F. (2018). Emerging roles of mitochondria in synaptic transmission and neurodegeneration. *Curr. Opin. Physiol.* 3, 82–93. doi: 10.1016/j.cophys.2018.03.009
- Lee, A., Kondapalli, C., Virga, D. M., Lewis, T. L. Jr., Koo, S. Y., Ashok, A., et al. (2022). Abeta42 oligomers trigger synaptic loss through CAMKK2-AMPK-dependent effectors coordinating mitochondrial fission and mitophagy. *Nat. Commun.* 13:4444. doi: 10.1038/s41467-022-32130-5
- Lewis, T. L. Jr., Kwon, S. K., Lee, A., Shaw, R., and Polleux, F. (2018). MFF-dependent mitochondrial fission regulates presynaptic release and axon branching

### SUPPLEMENTARY TABLE 1

Fixation methods and outcomes. A table listing the fixation conditions and their outcomes for both *in vitro* and *in vivo* conditions in the paper.

### SUPPLEMENTARY FIGURE 1

A combination of PFA and GA maintains mitochondria morphology better than PFA alone in cultured NIH3T3 cells. (A) Representative NIH3T3 cells labeled with mt-YFP (green) and tdTomato (purple) imaged after fixation with 4% PFA in PBS. (B) Representative NIH3T3 cells labeled with mt-YFP (green) and tdTomato (purple) imaged after fixation with 2% PFA/0.075% GA in PBS. (C) Quantification of total mitochondrial area per cell showing that fixation with PFA alone causes mitochondrial fragmentation (mean  $\pm$  95% CI). (D) Quantification of individual mitochondria for circularity shown as mean  $\pm$  95% CI before and after fixation with the indicated fixative solution. Mann–Whitney test.  $n_{4\%PFAcells} = 19$  cells,  $n_{PFA/GAcells} = 18$  cells,  $n_{4\%PFAcircularity} = 1,347$  mitochondria, and  $n_{PFA/GAcircularity} = 1,400$  mitochondria. \*\*\* $p < 0.001$ , \*\*\*\* $p < 0.0001$ . Scale bar, 25  $\mu$ m.

### SUPPLEMENTARY FIGURE 2

*In utero* electroporation strategy for sparse labeling of cortical neurons *in vivo*. A "DIO" plasmid encoding mitochondrial targeted mScarlet and cytoplasmic Venus was mixed with a low concentration of a second plasmid encoding Cre and then electroporated in E15.5 pups to give sparse labeling of cortical neurons *in vivo*.

### SUPPLEMENTARY FIGURE 3

p- $\alpha$ -Synuclein staining in different fixation solutions.  $\alpha$ -Synuclein accumulation was confirmed with p- $\alpha$ -synuclein staining. Both in control and  $\alpha$ -synuclein treated samples, 2% PFA/0.075% GA-fixed images showed higher background signals compared to 4% PFA or 4% PFA/4% sucrose fixatives. Scale bar, 20  $\mu$ m.



- by limiting axonal mitochondria size. *Nat. Commun.* 9:5008. doi: 10.1038/s41467-018-07416-2
- Lewis, T. L. Jr., Turi, G. F., Kwon, S. K., Losonczy, A., and Polleux, F. (2016). Progressive decrease of mitochondrial motility during maturation of cortical axons in vitro and in vivo. *Curr. Biol.* 26, 2602–2608. doi: 10.1016/j.cub.2016.07.064
- Lin, Y., Li, L. L., Nie, W., Liu, X., Adler, A., Xiao, C., et al. (2019). Brain activity regulates loose coupling between mitochondrial and cytosolic Ca(2+) transients. *Nat. Commun.* 10:5277. doi: 10.1038/s41467-019-13142-0
- Matheoud, D., Sugiura, A., Bellemare-Pelletier, A., Laplante, A., Rondeau, C., Chemali, M., et al. (2016). Parkinson's disease-related proteins PINK1 and Parkin repress mitochondrial antigen presentation. *Cell* 166, 314–327. doi: 10.1016/j.cell.2016.05.039
- Montana, U. O. (2022). *Rodent brain perfusion*. Available online at: <https://www.umt.edu/research/LAR/sops/sop-perfusion.php> (accessed February 9, 2022).
- Owens, K., Park, J. H., Gourley, S., Jones, H., and Kristian, T. (2015). Mitochondrial dynamics: Cell-type and hippocampal region specific changes following global cerebral ischemia. *J. Bioenerg. Biomembr.* 47, 13–31.
- Popov, V., Medvedev, N. I., Davies, H. A., and Stewart, M. G. (2005). Mitochondria form a filamentous reticular network in hippocampal dendrites but are present as discrete bodies in axons: A three-dimensional ultrastructural study. *J. Comp. Neurol.* 492, 50–65. doi: 10.1002/cne.20682
- Qin, Y., Jiang, W., Li, A., Gao, M., Liu, H., Gao, Y., et al. (2021). The combination of paraformaldehyde and glutaraldehyde is a potential fixative for mitochondria. *Biomolecules* 11:711. doi: 10.3390/biom11050711
- Rangaraju, V., Lauterbach, M., and Schuman, E. M. (2019). Spatially stable mitochondrial compartments fuel local translation during plasticity. *Cell* 176, 73–84.e15. doi: 10.1016/j.cell.2018.12.013
- Rolfe, D. F., and Brown, G. C. (1997). Cellular energy utilization and molecular origin of standard metabolic rate in mammals. *Physiol. Rev.* 77, 731–758.
- Swerdlow, R. H., Burns, J. M., and Khan, S. M. (2014). The Alzheimer's disease mitochondrial cascade hypothesis: Progress and perspectives. *Biochim. Biophys. Acta* 1842, 1219–1231.
- Turner, N. L., Macrina, T., Bae, J. A., Yang, R., Wilson, A. M., Schneider-Mizell, C., et al. (2022). Reconstruction of neocortex: Organelles, compartments, cells, circuits, and activity. *Cell* 185, 1082–1100.e24. doi: 10.1016/j.cell.2022.01.023
- Uhlig, C., Krause, H., Koch, T., Gama de Abreu, M., and Spieth, P. M. (2015). Anesthesia and monitoring in small laboratory mammals used in anesthesiology, respiratory and critical care research: A systematic review on the current reporting in top-10 impact factor ranked journals. *PLoS One* 10:e0134205. doi: 10.1371/journal.pone.0134205
- Wang, X., Su, B., Lee, H. G., Li, X., Perry, G., Smith, M. A., et al. (2009). Impaired balance of mitochondrial fission and fusion in Alzheimer's disease. *J. Neurosci.* 29, 9090–9103.
- Wu, J., Cai, Y., Wu, X., Ying, Y., Tai, Y., and He, M. (2021). Transcardiac perfusion of the mouse for brain tissue dissection and fixation. *Bio Protoc.* 11:e3988. doi: 10.21769/BioProtoc.3988
- Wu, W., Lin, C., Wu, K., Jiang, L., Wang, X., Li, W., et al. (2016). FUNDC1 regulates mitochondrial dynamics at the ER-mitochondrial contact site under hypoxic conditions. *EMBO J.* 35, 1368–1384. doi: 10.15252/embj.2015.93102
- Zhang, L., Trushin, S., Christensen, T. A., Bachmeier, B. V., Gateno, B., Schroeder, A., et al. (2016). Altered brain energetics induces mitochondrial fission arrest in Alzheimer's disease. *Sci. Rep.* 6:18725. doi: 10.1038/srep18725
- Zheng, X., Qian, Y., Fu, B., Jiao, D., Jiang, Y., Chen, P., et al. (2019). Mitochondrial fragmentation limits NK cell-based tumor immunosurveillance. *Nat. Immunol.* 20, 1656–1667. doi: 10.1038/s41590-019-0511-1
- Zhou, X., Chen, H., Wang, L., Lenahan, C., Lian, L., Ou, Y., et al. (2021). Mitochondrial dynamics: A potential therapeutic target for ischemic stroke. *Front. Aging Neurosci.* 13:721428. doi: 10.3389/fnagi.2021.721428